Estimating Foundation Water Vapor Release Using a Simple Moisture Balance and AIM-2: Case Study of a Contemporary Wood-Frame House

C.R. Boardman
Associate Member ASHRAE

Samuel V. Glass, PhD
Associate Member ASHRAE

Charles G. Carll

ABSTRACT

Proper management of indoor humidity in buildings is an essential aspect of durability. Following dissipation of moisture from construction materials, humidity levels during normal operation are generally assumed to primarily depend on the building volume, the number of building occupants and their behavior, the air exchange rate, and the water vapor content of outdoor air. A potentially large additional source of indoor humidity that often is not considered is the building foundation, which is in contact with earth that commonly is damp. Recent work has suggested that the rate of water vapor release from foundations may vary with season, with foundation temperature, and with indoor humidity.

This work presents results from a casestudy of a house with a wood foundation system in which we estimate foundation moisture release given basic interior and exterior conditions, such as relative humidity, temperature, and wind speed. The Alberta air infiltration model was calibrated using tracer gas measurements in the house and used to model air exchange. We use a simplified moisture balance model to estimate the hourly rate of foundation moisture release from the basement. This rate is presented and shown to correlate with stack-driven air exchange for this wood foundation system.

INTRODUCTION

Indoor humidity is an important moisture load for residential buildings in cold climates. High indoor moisture levels can lead to window condensation, mold growth, moisture accumulation in walls, poor indoor air quality, corrosion, and loss of thermal resistance in wet insulation. In the first year or two after construction, significant moisture sources in buildings may include moist building materials, such as framing lumber, wet-applied insulation, and especially recently poured concrete. Following dissipation of moisture from construction materials, humidity levels during normal operation vary and primarily depend on the number of building occupants, occupant behavior, air exchange rate, water vapor content of outdoor air, and the manner in which air exchange occurs. Common moisture sources include respiration and transpiration of humans, pets, and plants; showering and bathing; cooking; cleaning; and mechanical humidification. A potentially large additional moisture source, which is the focus of this study, is the building foundation, which is in contact with earth that commonly is damp or even wet (Christian 2009). Recent work suggests that the rate of water vapor release from foundations may vary with season, with foundation temperature, and with indoor humidity (Glass and TenWolde 2009; Kalamees et al. 2006; TenWolde and Pilon 2007). Better characterization of foundation moisture sources will improve estimates of the boundary conditions used in heat, air, and moisture (HAM) models (Kumaran and Sanders 2008).

A dual-purpose research and demonstration house was constructed in 2001 on the campus of the Forest Products Laboratory in Madison, WI. The building is referred to in this manuscript as the "FPL R-Demo" house. The building is not occupied but generally has been humidified during the heating season to simulate occupancy. Carll et al. (2007) describe the building's construction history, operation, and performance through the first five heating seasons. The primary focus of the work described by Carll et al. (2007) was

***C.R. Boardman** is a general engineer, **Samuel V.Glass** is a research physical scientist, and **Charles G. Carll** is a research forest products technologist at the Forest Products Laboratory (FPL), USDA Forest Service, Madison, WI.*

© 2010 ASHRAE

seasonal accumulation of moisture in walls when the building was operated during the heating season at or near indoor humidity design levels calculated by a method outlined in *ANSI/ASHRAE Standard 160-2009, Criteria for Moisture-Control Design Analysis in Buildings* (ASHRAE 2009). The calculation methodology in ASHRAE Standard 160 is based on an assumed moisture production rate in the house, assumed air exchange rate between the house and the outside, and water vapor content of outdoor air (TenWolde and Walker 2001).

For the first two heating seasons, the FPL R-Demo house was not actively humidified, but indoor humidity levels approaching design levels were nonetheless reached. The building was humidified to design levels for the third and fourth heating seasons, generally at substantially lesser rates of moisture release from humidifiers than the assumed release rate from which design humidity levels were calculated. For the fifth, sixth, seventh and eighth heating seasons, a set amount of moisture (10 kg/day) was released by humidification equipment into the house. This release rate was two-thirds of the assumed design rate of 15 kg/day (based on an assumed five occupants in the four-bedroom house), but design relative humidity (RH) levels were commonly reached and in some cases exceeded. The most probable explanation for these observations is that moisture enters through the foundation (Carll et al. 2007). This manuscript reports work done to quantify the rate of moisture release by the basement.

Moisture release by the basement was not well understood because of the unusual nature of the foundation in the house. The basement was constructed using a permanent wood foundation. Figure 1 shows the floor and wall detail. In the FPL R-Demo house, instead of a concrete slab the basement floor is plywood on 2 × 4 lumber, which rests on a black 0.15 mm (6 mil) polyethylene vapor retarder, which sits on gravel. Similarly, the basement walls are finished with gypsum interior attached to 2 × 8 lumber and exterior plywood sheathing, Outside, the sheathing is the same black plastic vapor retarder and gravel backfill. The basement floor area is 102 m^2 (1100 ft^2) with 112 m^2 (1200 ft^2) wall area and a volume of 280 m^3 (9900 ft^3), The total house volume (above and below grade) is 796 m^3 (28,100 ft^3).

In the investigation described in this manuscript, a moisture balance calculation methodology was developed to obtain an approximately continuous estimate of water vapor release from the building's foundation over the latter part of the eighth heating season, the subsequent spring, summer (cooling), and autumn seasons, and the beginning of the ninth heating season. The estimate was primarily based on three inputs: (1) humidity ratios of indoor and outdoor air, (2) continuous estimates of air exchange rates using a widely cited air-exchange model (with the model "tuned" based on tracer gas measurements), and (3) quantified amounts of either moisture release from humidifiers or collected condensate from the air conditioner's evaporator coil (during relevant seasons). The relationship between estimated water vapor release or capture by the foundation, soil moisture, foundation temperature, and indoor humidity was investigated. The moisture balance modeling methodology presented in this manuscript uses common measurements and models that are simple to implement. The methodology can thus be applied to other buildings.

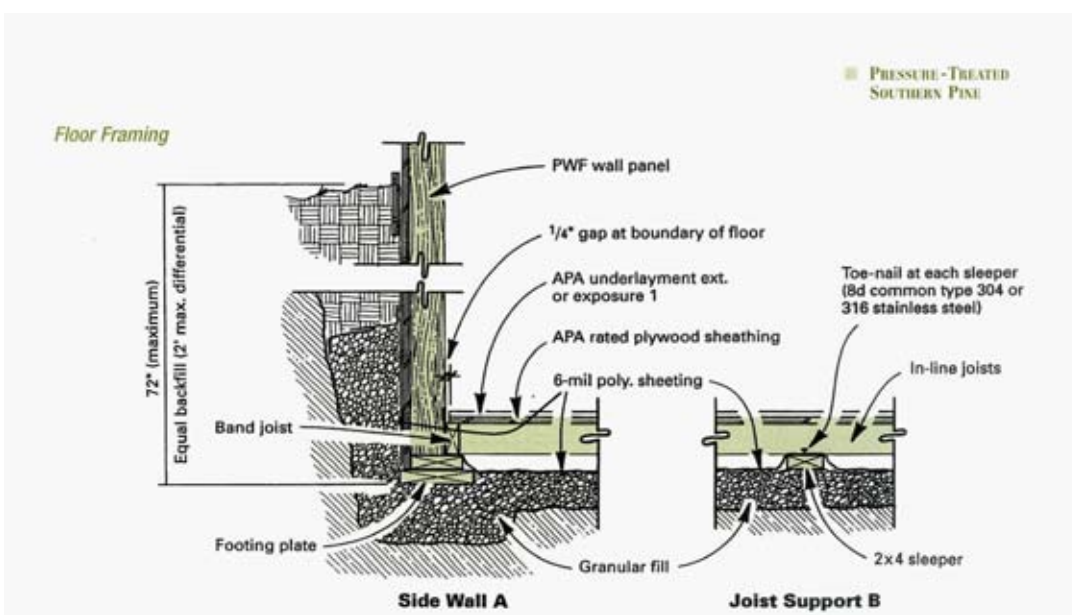

Figure 1 *FPL R-Demo house basement floor and wall details.*

MOISTURE BALANCE MODEL

The mathematical model developed for calculating foundation water vapor release is a variation of the mass balance used by TenWolde (1994). In this case, moisture generation in the house minus moisture leaving through air exchange and vapor diffusion through the building envelope equals the rate of moisture vapor mass change in the house air. Terms for short-term moisture sorption and condensation are included. The only condensation considered significant is that from the air conditioner. Information about the moisture accumulating in the walls during winter months is used to estimate vapor diffusion through the wall, since it is not negligible for the FPL R-Demo house. In this model two contributions to moisture generation are assumed: that from the foundation, which may also include long-term sorption, and that introduced using the humidifier to simulate occupant activities during the winter months (10 kg/day, October through April). These moisture flow terms are illustrated in Figure 2. Thus,

$$\rho V \frac{dw_{in}}{dt} = m_{gb} + m_{gh} - m_{na} - m_{mv} - m_d - m_{sorp} - m_c \qquad (1)$$

where

ρ = air density[1], kg/m³ (lb/ft³)

V = volume of house, m³ (ft³)

w_{in} = humidity ratio indoor air, mass of water vapor per mass of dry air

t = time, s (h)

m_{gb} = rate of moisture transport into basement, kg/s (lb/h)

m_{gh} = rate of moisture added through humidification, kg/s (lb/h)

m_{na} = rate of moisture loss through natural air exchange, kg/s (lb/h)

m_{mv} = rate of moisture loss through mechanical ventilation, kg/s (lb/h)

m_d = rate of moisture loss through diffusion, kg/s (lb/h)

m_{sorp} = rate of moisture loss through sorption7 kg/s (lb/h)

m_c = rate of moisture loss through condensation on cold surface, kg/s (lb/h)

The mass rate of change in the indoor humidity ratio is approximated numerically for a 1 hour time step Δt as

$$\frac{dw_{in}}{dt} \approx \frac{w_{in}^{t} - w_{in}^{t-1}}{\Delta t} \qquad (2)$$

where w_{in}^{t} and w_{in}^{t-1} are the indoor humidity ratios for the current and previous hours, respectively. The indoor humidity ratio and all mass flow rates in Equation 1, which are time

1. Air density is, of course, not constant as assumed in this moisture balance, but rather a function of temperature and pressure. However, throughout the year, room temperature variations changed the air density by less than 3%, and air pressure variations changed the air density by less than 2%.

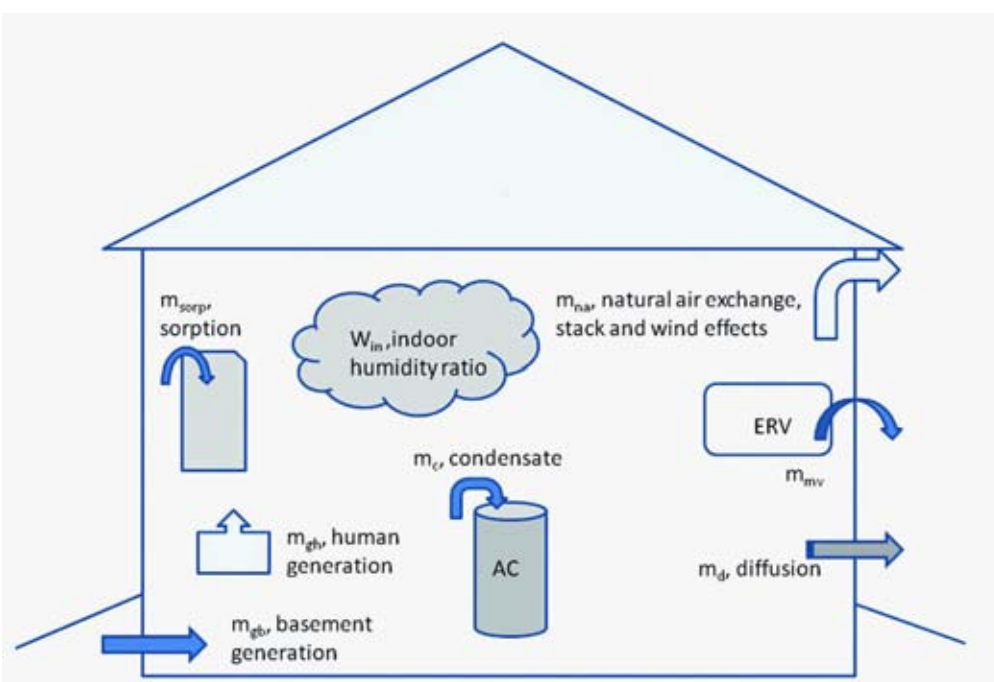

Figure 2 *Moisture balance terms.*

dependent, are also approximated numerically using a single value for each hour.

The dominant factor in this model for moisture loss during winter is the natural air exchange term m_{na}, primarily driven by the stack effect. The model uses the Alberta air infiltration model (AIM-2) (Walker and Wilson 1998) to calculate the natural air exchange rate. In the case of the FPL R-Demo house, calculation of the overall air exchange rate and calculation of moisture exchange associated with air exchange was complicated by the presence (and use) of an Energy Recovery Ventilator (ERV). The m_{mv} term was, therefore, added to estimate the moisture loss rate associated with the operation of the ERV, which is discussed in greater detail later in this manuscript, as are the terms in Equation 1 for diffusion and sorption. The condensation term m_c was assumed negligible except for air-conditioner condensate, which was measured hourly using a tipping bucket during the end of the cooling season.

Natural Air Exchange

AIM-2 is a simple single-zone model for predicting building air infiltration. It was used successfully by Wang et al. (2009) to predict natural air exchange in a sample of single-family houses. The model relies on the indoor-outdoor temperature difference and wind speed to predict infiltration from the stack effect and wind driven exchange; it also relies on house characteristics that can be derived from a blower door test (ASTM 2003) and estimates of the location of envelope air leakage. An overview of the AIM-2 model is provided by Wang et al. (2009), and details can be found in Walker and Wilson (1998). Some of the core equations are outlined here so that data input values can be understood. The total air infiltration rate, Q_{aim}, is the sum of the infiltration rate from stack effect, Q_s, and infiltration rate from wind, Q_w, as calculated in Equation 3.

$$Q_{aim} = [Q_s^{1/n} + Q_w^{1/n} - 0.33(Q_s Q_w)^{1/2n}]^n \quad (3)$$

Both Q_s and Q_w depend, in part, on the building envelope flow coefficient, C, and the flow exponent, n, determined by blower door testing. They are calculated as

$$Q_s = CF_s\left[\rho g H\left(\frac{T_{in} - T_{out}}{T_{in}}\right)\right]^n \quad (4)$$

$$Q_w = CF_w\left[\frac{\rho}{2}(S_w U)^2\right]^n \quad (5)$$

where

g = acceleration due to gravity, m/s² (ft/m in²)
H = height of building at highest eave, m (ft)
T = temperatures in K (°R) inside (in) and outside (out)
S_w = wind shield factor to account for building microclimate, dimensionless
U = wind speed, m/s (mph)

And the respective units for Q_s, Q_w, C, and n are

Q_s m³/s (ft³/min)
Q_w m³/s (ft³/min)
C m³s⁻¹·Pa⁻ⁿ (ft³min⁻¹[in. Hg]⁻ⁿ)
n dimensionless exponent
F_s dimensionless flow factor for stack effect
F_w dimensionless flow factor for wind effect

The dimensionless flow factors F_s and F_w are calculated based on assumed leakage locations. There is no open flue for this house, so the leakage locations are distributed across the ceiling, walls, and floor. The leakage distribution and the wind shield factor, s_w, were optimized through fitting the relevant coefficients using measured air exchange rates in the house, determined by tracer gas testing as described below.

Calculating Moisture Loss from Natural Air Exchange, m_{na}

The moisture loss rate associated with natural air exchange, m_{na}, was calculated from the mass water vapor exchange rate by natural ventilation (derived from volumetric air exchange rate Q_{aim}, predicted by the AIM-2 model)[2].

$$m_{na} = Q_{aim}\left(\frac{P_{in} - P_{out}}{R_w T_{in}}\right) \quad (6)$$

where

R_w = gas constant for water vapor 461.5 J/kg·K (2760 ft·lb/slug·°R)
P = vapor pressure in Pa (in. Hg) of water at interior (in) and exterior (out)

Mechanical Ventilation

As indicated previously, the incorporation of an Energy Recovery Ventilator (ERV) in the R-Demo house and its use during essentially the entire calendar year 2009 complicated moisture balance calculations. Since the core of the ERV transfers both heat and moisture across its cellulose-based membrane, the actual moisture exchange associated with mechanical ventilation depends on the ERV moisture transfer effectiveness, as well as on its runtime[3]. Very little data exists that can be used to model ERV moisture transfer effectiveness. A study is underway to better characterize the ERV in the FPL R-Demo house. For purposes of this manuscript, a preliminary correlation of measured values between ERV effectiveness

2. This way of expressing the mass flow is approximately equivalent to the alternative formulation using the humidity ratio w in which $m_{na} = \rho Q_{aim}(w_{in} - w_{out})$ when P_{in} and P_{out} are similar and much smaller than atmospheric pressure.

3. Heat recovery ventilators and energy recovery ventilators commonly have flow rates in excess of 100 cfm and are commonly run on timers to avoid overventilation of the building. The ERV in this building was typically run one-third of the time by timer control (40 minutes in each two-hour period).

and average temperature and RH was used to determine the moisture exchange.

The mathematical simulation of moisture exchange is based on Barringer and McCugan (1988) and uses the humidity ratio (w). Then, numbering the four ports into the ERV as 1 for outside air going in, 2 for supply air to the house, 3 for inside air going into the ERV for exhaust, and 4 for actual exhaust air to outside (as illustrated in Figure 3), a mass balance in the core requires

$$w_1 m_1 + w_3 m_3 = w_2 m_2 + m_4 w_4 \tag{7}$$

where m_n is the mass flow rate in kg/s (lb/h) of dry air flowing through port n of the ERV.

The ERV moisture transfer effectiveness, ε_m, is defined as

$$\varepsilon_m = \frac{w_2 - w_1}{w_3 - w_1} \tag{8}$$

Here is it assumed that the ERV's airflows are perfectly balanced, so all the dry air mass flow rates, m_{da}, through the various ports of the ERV are equal, and the actual moisture loss rate, m_{mv} (kg/s [lb/h]), can be expressed as

$$m_{mv} = m_{da}(w_3 - w_2) = m_{da}(w_3 - w_1)(1 - \varepsilon_m) \tag{9}$$

Diffusion through Walls

In many houses water vapor diffusion can be ignored, but this house has no significant vapor barrier in the walls[4]. Diffusion through the ceiling is neglected because there is a polyethylene vapor barrier under the attic insulation. In the FPL R-Demo house, moisture accumulates in the walls in the cellulose insulation and the oriented strand board sheathing during the winter. For simulating the moisture balance of this house, the humidity model needed an estimate of m_d . A one-dimensional model of a wall consisting of painted gypsum board, cellulose fiber insulation, oriented strand board (OSB) sheathing, and a polyolefin weather resistive barrier was simulated using WUFI (IBP 2009). The FPL R-Demo house has a variety of cladding systems, two of which were included in the WUFI model—a northwest-facing brick veneer (with air gap) and a southeast-facing plywood panel siding (with no air gap). The simulation period was set to run for a calendar year beginning in January 2009. Hourly site-measured temperature and RH conditions for this calendar year were generally used for both interior and exterior conditions. For certain time periods during the course of the year, hourly conditions from the KMSN (local airport) weather station were used for exterior conditions. Exterior rain from the KMSN weather station and solar irradiance from the ASHRAE 2009 Clear Sky Model (Gueymard and Thevenard 2009) for Madison were included in the simulation.

Moisture content in the OSB sheathing of the brick-clad walls in the FPL R-Demo house was monitored hourly[5]. Initial

4. There is latex paint on the interior gypsum walls, but this does little to slow water vapor diffusion to the outside. Any water vapor diffusion through the basement walls is included in the basement generation term, m_{gb}.

5. Hourly monitoring was a continuation of the monitoring described in a previous manuscript (Carll et al, 2007). The instrumentation was still evidently functional during the simulation period.

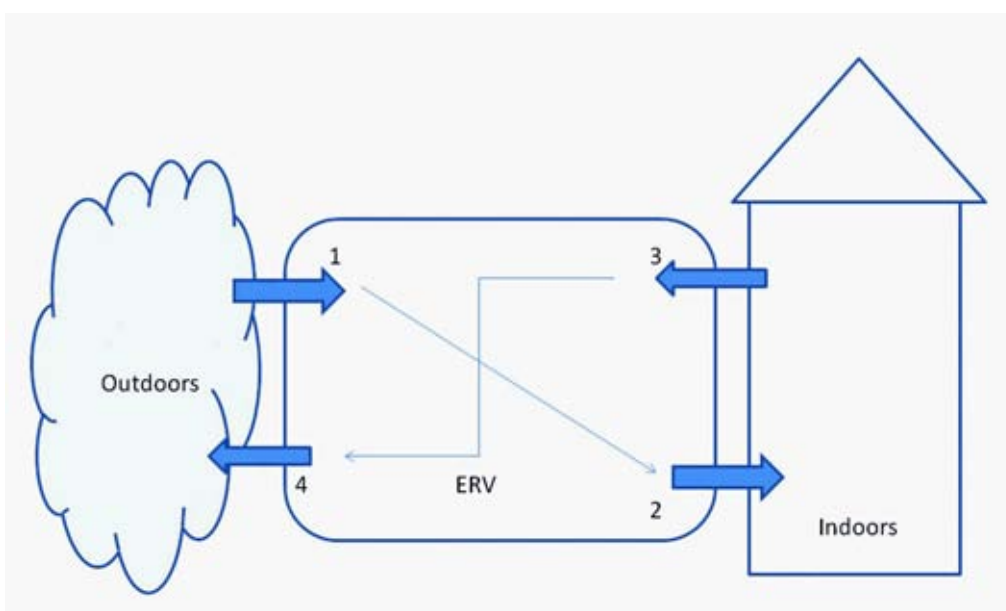

Figure 3 *ERV port numbers.*

conditions were set to correspondwithmeasuredconditions in the wall on January 1, 2009. The default material properties in the WUFI database of each wall layer were used. The air change rate in the air gap behind the brick was adjusted so that the model was able to track the measured drying behavior of the OSB in the instrumented wall during the spring. WUFI allows display ofthemoisture content in each layer and output of moisture flux at the interior surface. The hourly moisture flux at the gypsum wall surface scaled by the total wall area was used as m_d in the moisture balance model.

Sorption in Hygroscopic Materials

The sorption term, m_{sorp}, was calculated using an empirical sorption constant per unit of floor area, k (kg/s·m² [lb/h·ft²]) following the method of TenWolde (1994):

$$m_{sorp} = kA(RH - RH_w) \tag{10}$$

where

A = total floor area of the building, m² (ft²), 306.6 m² for R-Demo house

RH = indoor relative humidity, %

RH_w = weighted indoor relative humidity, an exponentially weighted time average ofprevious RH, %

This method of handling sorption was to account for short-term moisture storage in hygroscopic materials, which depends on the recent RH history. The value was experimentally determined for the FPL R-Demo house following the method used by TenWolde (1994) in which k is tuned to allow the predicted and actual RH to match given a known RH history, known history of air exchange, and assumed moisture generation[6]. The value used for k was 0.0972×10^{-6} kg/s·m² (0.072×10^{-3} lb/h·ft²), which is similar to that found by TenWolde (1994) and by Plathner et al. (1998).

MEASUREMENT EQUIPMENT

Tracer Gas Testing

Tracer gas testing allowed quantification of natural and mechanical air exchange rates in the house. Air exchange rates were quantified on 60 individual days. On some of the days, the ERV was operated, while on other days the ERV was inactive (and its ports blocked). Measured air exchange rates were compared with rates predicted by the AIM-2 model. The tracer gas technique utilized sulfur hexafluoride (SF6) as the tracer gas; tracer gas concentration was determined by electron capture chromatography. Exchange rates were determined by monitoring decay in the concentrations of tracer gas (as outlined in ASTM Standard E741-00) over the course of eight hours. The air change per hour (ach) in the R-Demo house was commonly around 0.2. The interval between measurements was typically 30 minutes, with 15 or more readings taken to allow multiple decay time periods to elapse. The furnace fan was set to run continuously during tracer gas tests, and free-standing "box" fans were placedoneach floor level to promote even distribution of the tracer gas. Tracer gas concentration was sampled on each floor of the house. The measurement equipment contains internal software that can calculate ach based on all concentration readings. This value was compared to ach values calculated for each sample location using the simple decay model:

$$C_f(t) = C_i e^{-nt} \tag{11}$$

So,

$$ach = n = \frac{1}{t}\ln\left(\frac{C_i}{C_f}\right) \tag{12}$$

where

C_i = initial SF6 concentration (typically in ppb)

C_f = fina1 SF6 concentration after

t = time in hours since start

n = decay constant which is the ach value

The ach values varied somewhat in time and location, so a weighted average was picked to represent the typical value for the house for a given test period. Air change rate values in the basement were usually higher than on first- or second-story levels. The weighted average used to represent the whole house was closest to the main floorreadings andtypicallywas within 0.03 ach of the other readings.

Calibrating the AIM-2 Model

Air change per hour values obtained from tracer gas tests on days when the ERV was disabled (and its ports blocked) were used to calibrate the AIM-2 model parameters. Since ach represents an average across an eight hour period, the hourly temperatures and wind speeds were averaged across the same period during which a tracer gas test was performed. The flow coeffcient and flow exponent (from blower door testing) were 0.0503 $m^3 \cdot s^{-1} \cdot Pa^{-0.679}$ (41,148 $ft^3 \cdot min^{-1}[in.\ Hg]^{-0.679}$)[7] and 0.679, respective1y. Eave height (H in Equation 4) was 5.49 m (1 8 ft). The air density (in Equations 4 and 5) was considered constant at a value of 1.15 kg/m³ (0.072 lb/ft³); this corresponds with density at room temperature and average atmospheric pressure at Madison.[8] Hourly site-measured indoor and outdoor temperatures and site-measured wind readings

6. For these calculations, RH history was weighted over a total of40 hours so the equivalent the constant was 10 hours. The actual RH tests were run over a number of days using a humidifier on the main floor to create the known moisture generation. The k value was not significantly sensitive to the the constant.

7. The more commonly given C value is 106.6 cfm $(Pa)^{-n}$

8. Room temperature was near 21°C (70°F) most of the winter, and average atmospheric pressure was 98439 Pa (29.1 in. Hg).

were typically used to derive test period average values for the relevant parameters in Equations 4 and 5. Site measured wind readings were taken at roof peak and so were close to wind speeds at eave height. At times when site-measured wind or outdoor temperature data were not available[9], data from the KMSN (nearest airport) weather station were substituted for site-measured data. Checks made at times when both airport and site-measured wind data were available indicated that wind speeds measured at the airport were higher than wind speeds measured on-site. Thus, when airport wind speeds were used in lieu of site-measured values, the values were reduced to 70% of the wind speed values reported by the weather service.

Calibrating the model amounted to optimization of the windshield factor, S_w (determinedto be 0.5), and optimization of F_s and F_w factors in Equations 4 and 5. Each of the F factors is associated with distribution of air leaks across the building envelope. Tuning of the AIM-2 model parameters resulted in a predicted distribution of leakage areas as follows: 37% in ceilings, 27% in floors, and 36% in walls. An overview of predicted (AIM-2 model) ach values versus measured values is presented in Figure 4. The figure includes data points from 39 tests performed with the ERV off and openings taped closed, and 21 tests performed with the ERV open and running at various duty cycles, usually one-third. The pressure difference between inside and outside was not extensively measured but was assumed small and roughly equivalent between the various ERV configurations, which were run during all seasons.

Once the AIM-2 model had been optimized for values of S_w, F_w, and F_s, the difference between ach determined by tracer gas testing with the ERV running and the ach values predicted by the AIM-2 model for the conditions that prevailed during the tracer gas test could be used to estimate the mechanical ventilation flow rate provided by the ERV. This was calculated as 0.0576±0.002 m³/s (122±5 cfm) when the ERV was running. Similar flows were directly measured using a vane anemometer in the incoming duct. On the one-third duty cycle, the ERV provided an estimated 0.1 ach.

ERV Moisture Transfer Effectiveness

The final step to calculation of m_{mv} for the R-Demo house required a value for the ERV moisture transfer effectiveness. To calculate ε_m, each input and exit duct from the ERV was outfitted with a humidity and temperature sensor. Sensor values were recorded every minute, and temperature and RH values were used to calculate the humidity ratio w for air flowing through each port. During the 40 minutes out of each 2 hours that the fans were running, the water vapor transfers (Equation 7) came within 3% of balance after the fan had run for 34 minutes and a steady-state condition had been achieved. Effectiveness could, in turn, be calculated for each

9. The wind instrument failed and was replaced during 2009, and the temperature and humidity sensors were removed for a period to check calibration.

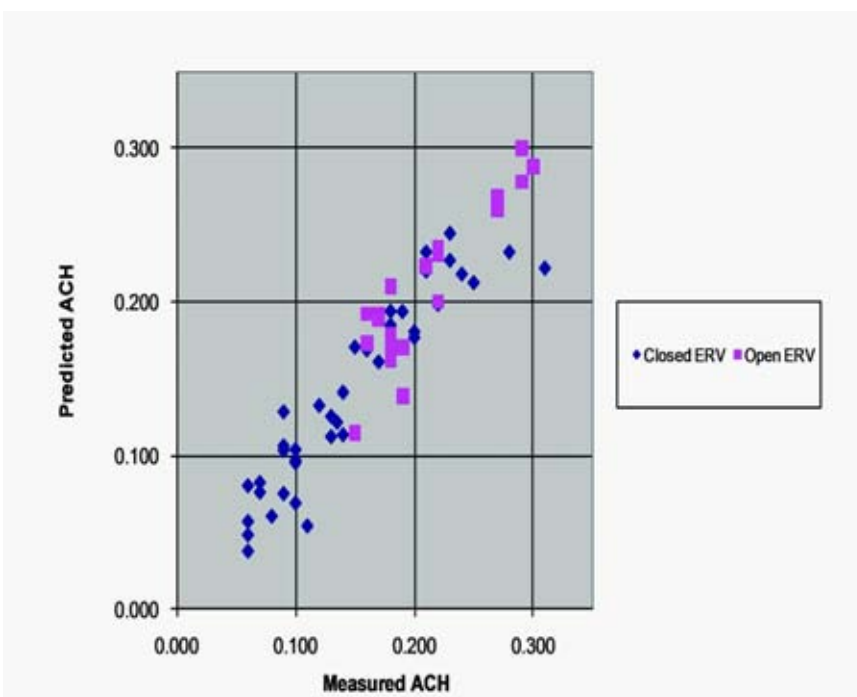

Figure 4 *Predicted achfrom AIM-2 versus measured achfrom tracer gas study.*

run cycle by averaging the effectiveness for each minute the fan ran after steady-state had been achieved. The first few minutes after the ERV fan starts up are a transition period during which time the effectiveness numbers may exceed 1; this apparently is the result of moisture storage in the core during the period when the ERV fans do not run. The ERV core had a wide range of moisture transfer effectiveness, and the effectiveness was fairly well correlated with the average RH. Figure 5 presents the measured effectiveness values versus RH_{ave} [10]. These data are fitted to an empirical formula so that effectiveness is calculated from the average temperature ($[T_{in} + T_{out}]/2 = T_{ave}$) and the average relative humidity ($[RH_{in} + RH_{out}]/2 = RH_{ave}$):

10. The effectiveness is in the range claimed by the manufacturer of the ERV.

$$\varepsilon_m = 0.178e^{(4.88RH_{ave}/T_{ave})} \tag{13}$$

where

RH = relative humidity, %

T = temperature, K

e = natural log

Figure 5 shows the fit of the empirical data to Equation 13 for which RH_{ave} and T_{ave} are the input parameters. The effectiveness goes up with RH as expected.

Additional Instrumentation

Bottom plates of the foundation walls were instrumented at 13 locations with moisture pins and type T thermocouples. Bottom-plate moisture contents showed essentially no seasonal variation but varied spatially. The building site was

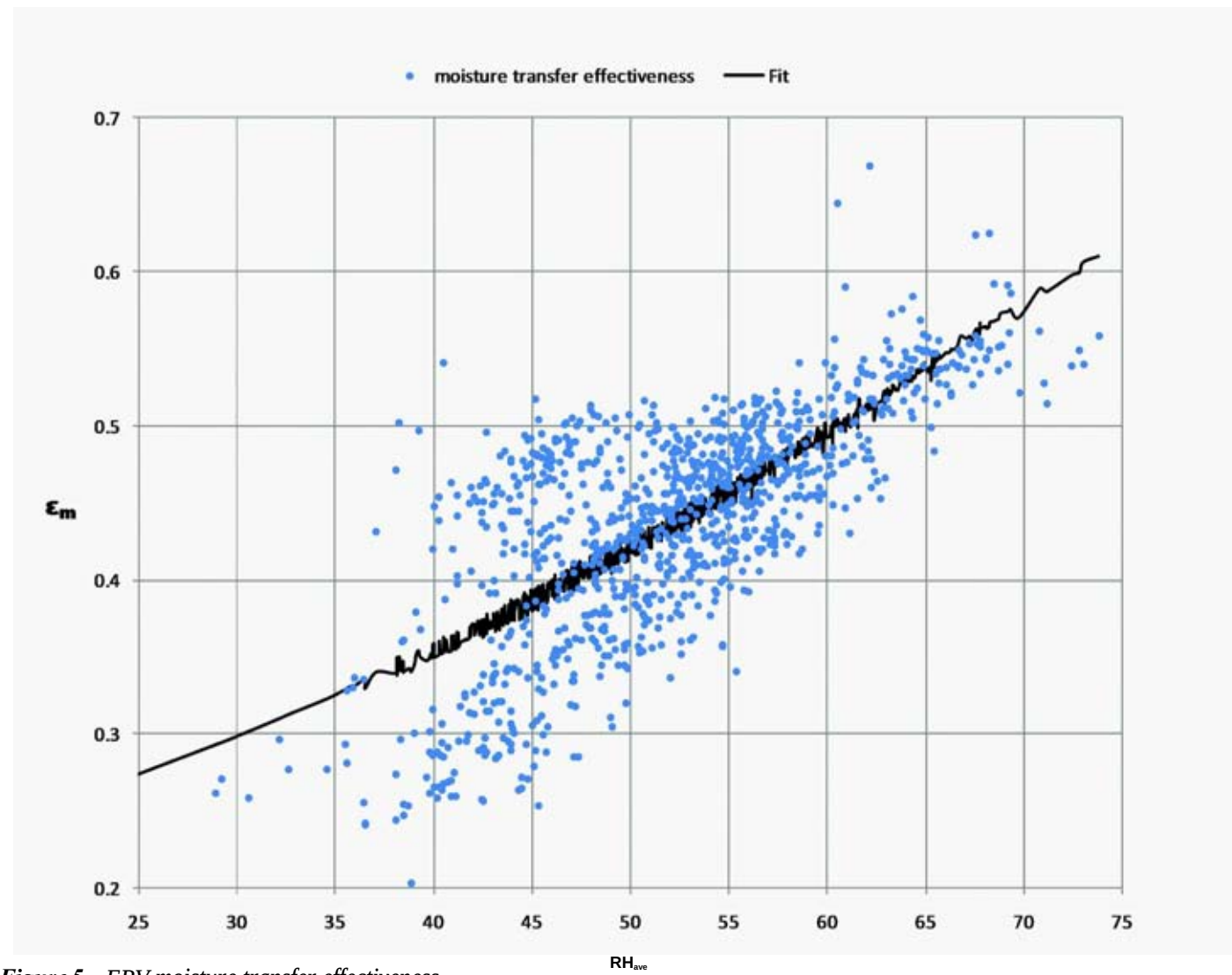

Figure 5 *ERV moisture transfer effectiveness.*

not level; foundation bottom plates on the "uphill" side of the building were chronically at or near fiber saturation (40% moisture content), whereas bottom plates on the "downhill" side of the building registered moisture contents near 20% (in approximate equilibrium with 90% RH). Two of the foundation bottom-plate locations were used to represent the basement foundation temperature. The depth of below-grade burial of the bottom plate at these locations was roughly 1.7 m (5.5 ft). This was less than the average burial depth for the foundation wall bottom plates for this building. Hourly temperature readings at these two locations were averaged. and a time plot of the values is shown in Figure 6.

RESULTS

Hourly moisture release for the last three months of the 2009 year is shown in Figure 7 with a five-day moving average. Daily moisture release for the 2009 year is shown in Figure 8 with a 14-day moving average. There was significant variation in the hourly values, with somewhat less variability in the daily summaries. This variability was primarily a result of the air exchange, which dominates the moisture balance. In Figure 9, the hourly values of $m_{na} + m_{mv}$ and m_{sorp} show the relative contribution and variability of these terms in the moisture exchange for a week in October during which the diffusion term m_d was always less than 0.1 kg/h and there was no contribution from m_c or m_{gh} .

A significant yearly trend observable in Figure 8 was that the foundation moisture release rate was largest during the heating season. The daily rate was around 20 kg/day (44.1 lb/day) in January and early February, dropped below 20 kg/day for most of February and March, and moved significantly below 10 kg/day in mid April. The foundation moisture release rate had a value near zero only during late spring and the summer months; the rate began climbing again in October.

DISCUSSION

The primary correlation found in this investigation was between foundation moisture release and season. Given adequate soil moisture and foundation temperature. water vapor entered the basement through the All-Weather Wood Foundation system carried by air infiltration through the gravel on which the foundation rests. The air exchange was dominated by

Figure 6 *Wood foundation bottom plate temperature.*

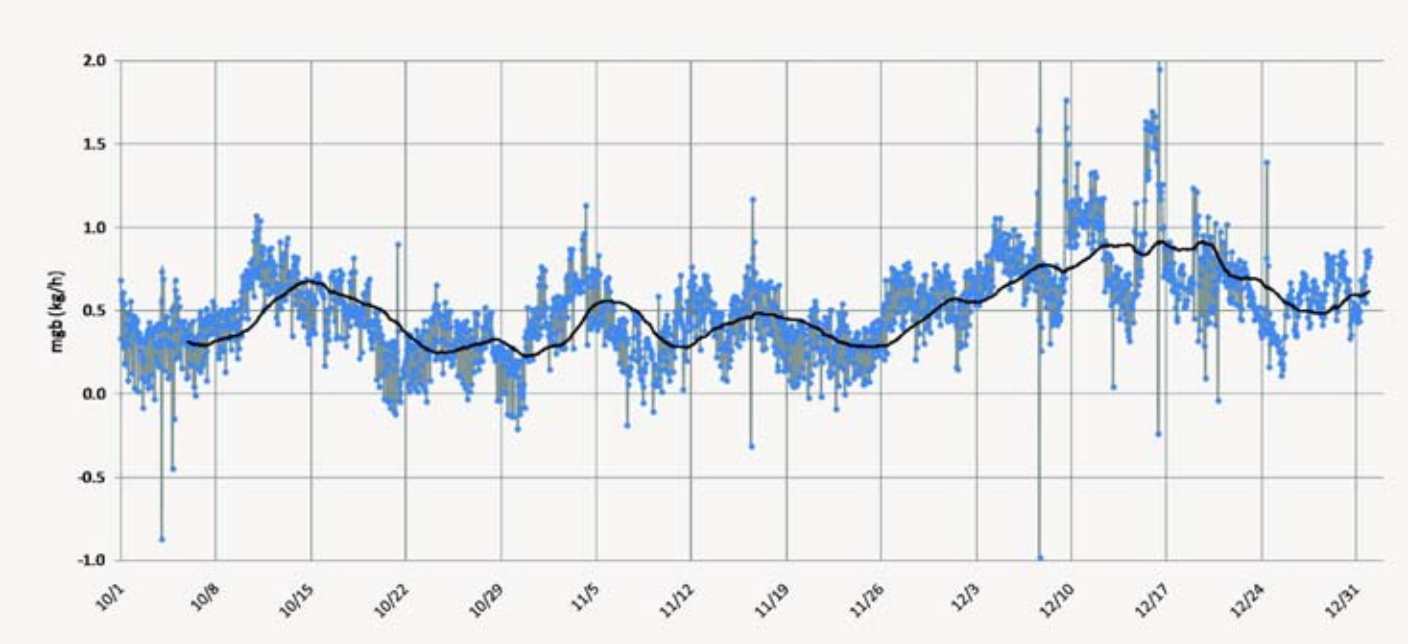

Figure 7 *Moisture transport into basement (kg/h) with 5 day moving average.*

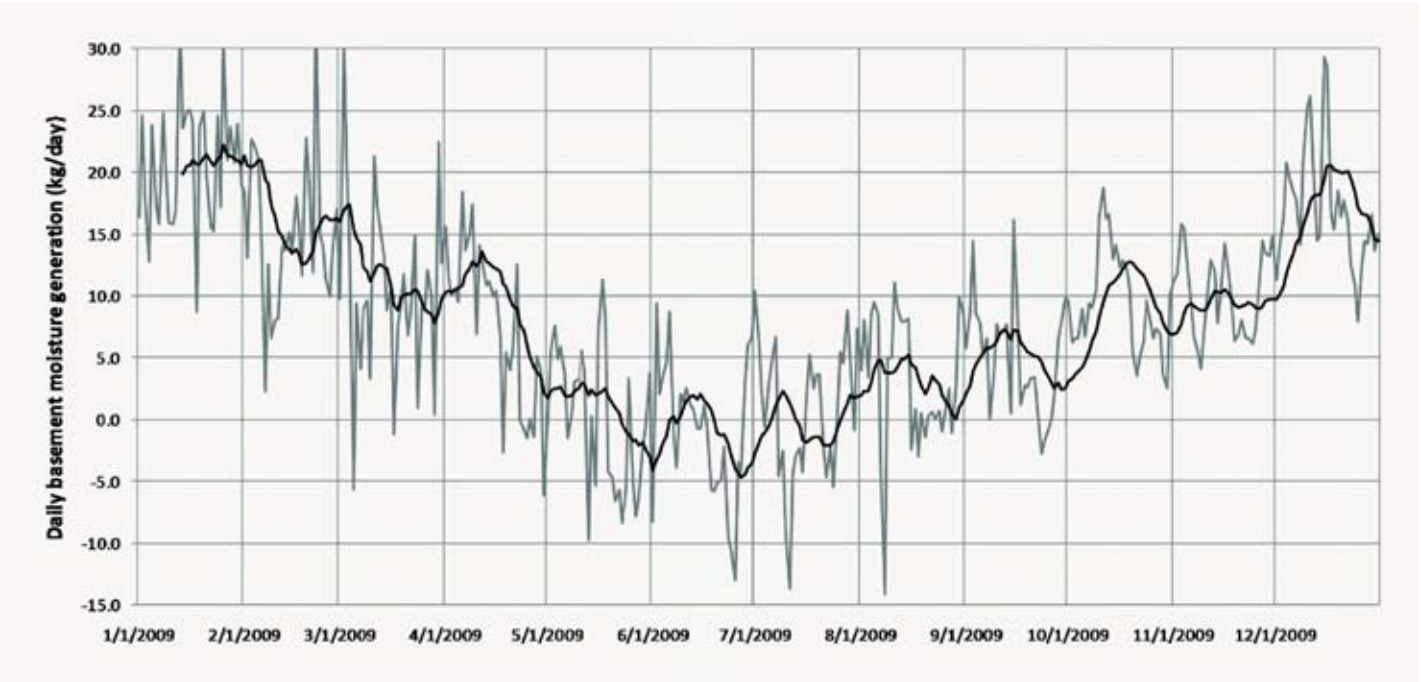

Figure 8 *Moisture transport into basement (kg/day) with 14 day moving average.*

the stack effect. which was large during the heating season. Figure 10 shows good correlation between the foundation moisture release rate and the moisture loss calculated using only the stack-effect-driven air exchange. This result provides support for (and a rate estimate of) Quirouette's suggestion (1983) that in specific cases, foundation moisture release could be dominated by air infiltration through the basement. The wood foundation could also be a site for long-term moisture sorption, so the foundation moisture release calculated in this manuscript includes an unknown contribution from long-term sorption or desorption of wood members. This aspect needs further study along the lines of those explored by Plathner et al. (1998), who introduced a long-term sorption constant in addition to the short-term sorption constant (similar to k in Equation 10) but

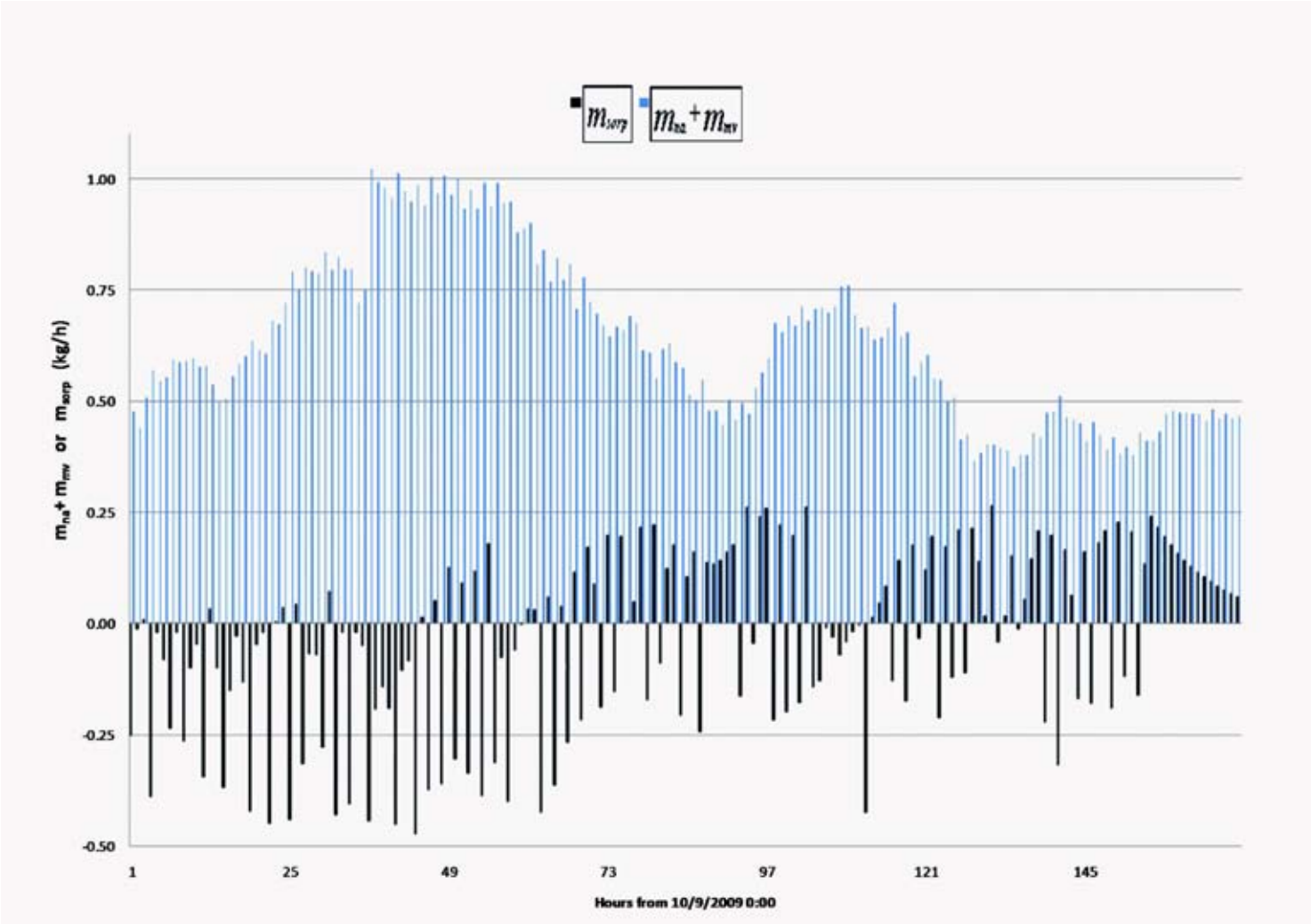

Figure 9 *Hourly contributions to moisture transport by sorption and airflow.*

with a longer time period for the RH weighted average. However, recent work by Kurnitski et al. (2007) suggests that any long-term effect could be small enough to be negligible.

Figure 6 shows a seasonal trend in foundation bottom-plate temperature that is distinctly out of phase with calculated foundation moisture release (Figure 8). The lowest temperature values. however. which occur mid-March. do not fall substantially below 10°C (50°F). Water at saturation at 10°C exerts a vapor pressure of roughly 1280 Pa, a value typically in excess of indoor vapor pressure in the building during winter months. Ground temperatures near basement floor level thus appear sufficient to evaporate moisture into basement air, provided that the ground is amply moist. The measured foundation bottom-plate moisture contents suggest that this is the case. The ample supply of soil moisture year round at basement floor level concurs with the research literature on soil moisture climatology in the Midwestern United States (Hollinger and Isard 1994; Robock et al. 2000). Figure 11 compares the vapor pressure of moisture in the basement air over the 2009 year with the estimated vapor pressure of moisture in the soil and gravel outside the foundation, assuming the air is saturated and at the foundation base plate temperature. This indicates the soil is always an available moisture source[11].

Taking 15 kg/day as the value for foundation moisture release in the FPL R-Demo house on a typical winter day allows comparison to other investigations. Christian (2009) suggests a design target of 3 kg/day for foundation moisture load but notes examples of foundations that are significantly higher, giving the range as 0–50 kg/day. On a square-meter floor-area basis, the R-Demo house produced 0.147 kg/day m^2, which is about 7 times that found for the concrete boxes extensively studied at the Foundation Test Facility in Minnesota, which produced 0.02 kg/day·m^2 (FTF 1999)[12]. It should be

[11] The polyethylene that wraps the basement floor and walls may be effective as a vapor barrier but is apparently ineffective as an air barrier, since it has holes and the seams were not taped.

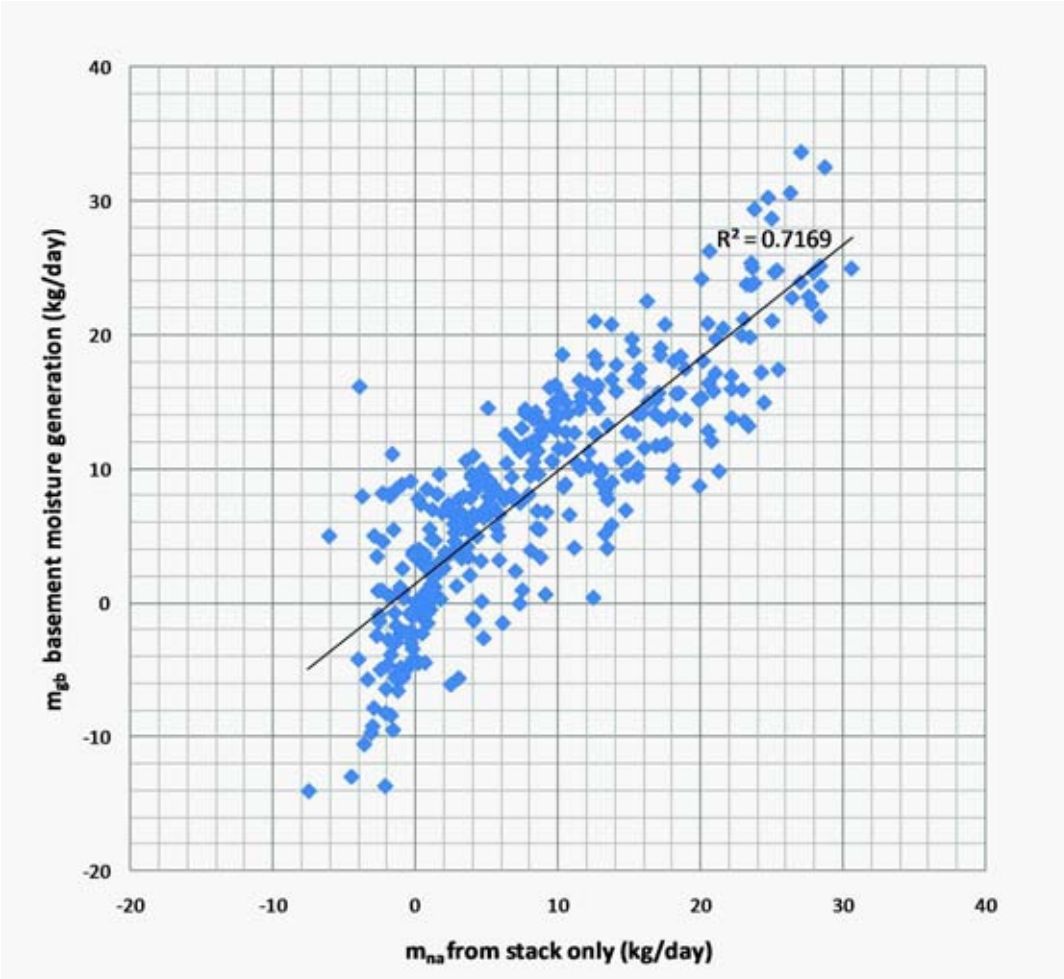

Figure 10 *Correlation of total basement moisture transport with moisture loss due to stack effect.*

noted, however, that the modules studied at the FTF did not have actual buildings of single- or two-story height erected over them, and the "guard" sections that were erected over the modules were effectively isolated from the modules with uninterrupted "floor" systems constructed of structural insulated panels. The FTF modules were, thus, unlike the foundation of this building, largely isolated from building stack effects. The masonry foundation systems studied at the FTF may also behave differently than treated wood foundations systems, particularly with regard to air leakage characteristics.

The overall measurement uncertainty in this investigation was difficult to estimate given the large number of terms involved in the calculation. The air exchange rate measured with tracer gas testing was well defined with error, at most, 0.03 out of a typical 0.2 ach, so around 15%. The AIM-2 prediction for air exchange had root-mean-square error of only 0.024 ach. Many of the other terms are small. For example, the typical maximum m_d for any hour was 0.3 kg, and the value was typically less than 20% of m_{na} . The largest m_{sorp} values were at most 3.3 kg/h and occurred during summer, when the daily release rate was low. Typically m_{sorp} contributed less than 10% to the total moisture release in a day. The total amount of moisture added manually, m_{gh} , was known to within a few percent. The uncertainty in that term was when during the day that release occurred, so it contributed to uncertainty in hourly variation but not the daily total. The m_c term was often significant during the summer but was good to within 0.01 kg/h during the period it was measured. That data was not available for June and early July 2009. Since these other terms are small, the primary uncertainty in basement moisture release rate was from m_{na} .

A sensitivity analysis was performed on the moisture loss rate attributable to natural air exchange, m_{na}, to get a feel for how different inputs affected the moisture exchange. The results are most sensitive to indoor RH. To quantify the effect of changing RH values, a bracketing scenario was considered for each of four selected winter days to see the

[12.] This calculation assumes a typical rate of 0.75 kg/day for the 37.2 m² basement floor area of the FTF North reference.

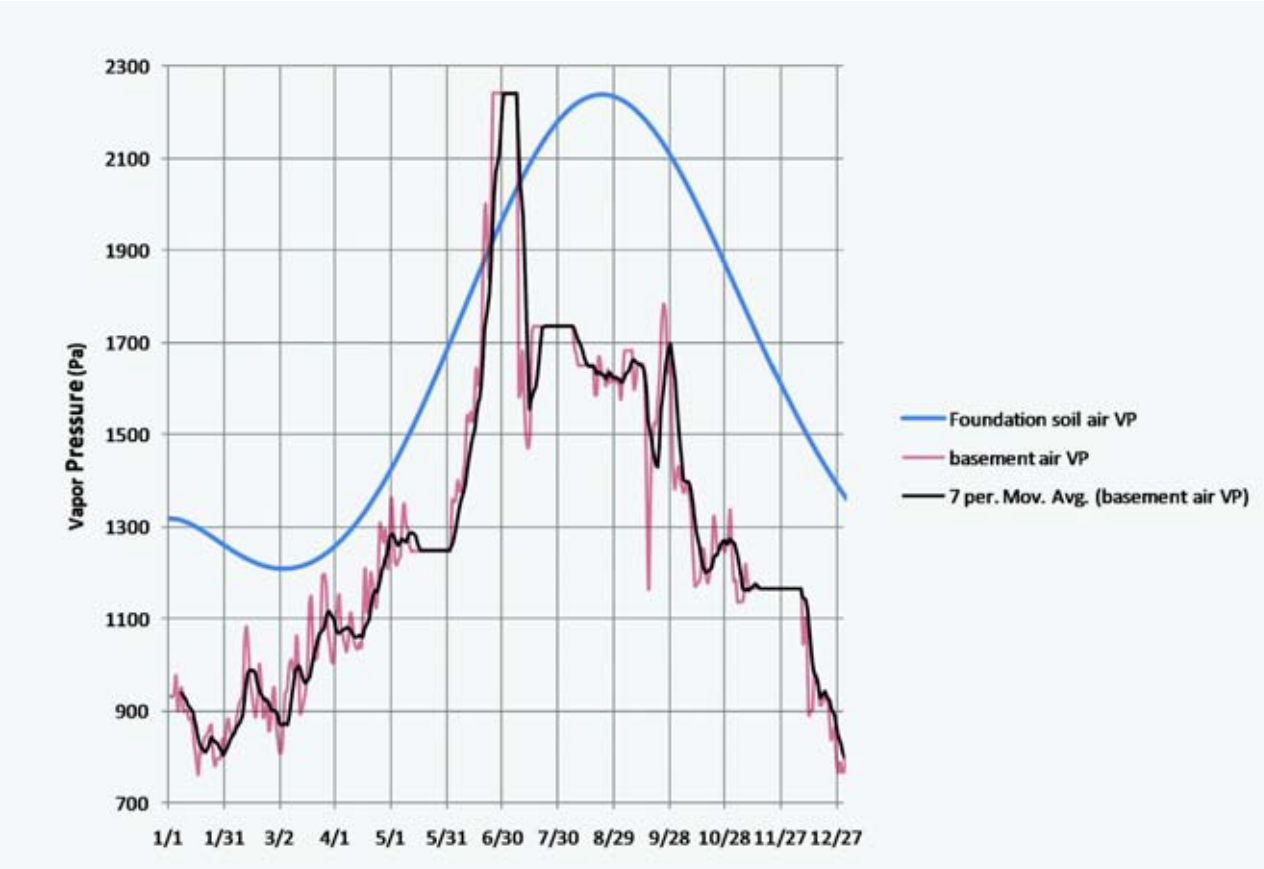

Figure 11 *Vaporpressure of soil moisture and basement air*

effect of increasing and decreasing moisture exchange through changing the driving terms in the AIM-2 model. At one extreme (to represent a clear over-estimate of m_{na}), the hourly wind speed values were increased by 1 mph, the outdoor temperature was decreased by 1°F, the indoor RH was increased by 1 %, and the outdoor RH was decreased by 1 %. At the other extreme (to represent a clear underestimate of m_{na}), the wind speed values were decreased by 1 mph, the outdoor temperature was increased by 1°F, the indoor RH was decreased by 1 %, and the outdoor RH was increased by 1 %. Under this bracketing scenario, the daily values for basement moisture release were 20±3 kg for October 11, 16±3 kg for November 18, 15±3 kg for November 27, and 27±3 kg for December 11. Thus, the uncertainty in basement moisture release rate was 20% or less, even when all inputs pushed the combined error in the same direction.

CONCLUSION

Foundation moisture release in the FPL R-Demo house has been found to correlate best with stack-driven air exchange. The water vapor release rate into the building from the "foundation system" (consisting of the wood foundation itself as well as the surrounding gravel and soil) is typically 10–20kg/day (22-44 lb/day) during the heating season, which is significantly higher than typical rates in concrete/masonry block basements driven by diffusion. On most days during cold weather this exceeds the assumed interior moisture production rate estimated by ASHRAE Standard 160 for a residential building of this size, yet the basement RH stays in an acceptable range without active dehumidification.

ACKNOWLEDGMENTS

The authors acknowledge the support of the Forest Products Laboratory (FPL) in carrying out this work. We thank Robert Munson of FPL for data maintenance and compilation. The paper was improved by helpful comments from Anton TenWolde (retired FPL research physicist), Collin Olson (staff physicist, Energy Conservatory), and three anonymous reviewers.

REFERENCES

ASHRAE. 2009. *ANSI/ASHRAE Standard 160-2009, Criteria for Moisture-Control Design Analysis in Buildings.* Atlanta: American Society of Heating, Refrigerating and Air-conditioning Engineers, Inc.

ASTM. 2003. *Designation E779-03, Standard Test Method for Determining Air leakage Rate by Fan Pressurization.* West Conshohocken, PA: ASTM International.

ASTM. 2006. Designation E741-00, Standard Test Method for Determining Air Change in a Single Zone by means of a Tracer Gas Dilution. West Conshohocken, PA: ASTM International.

Barringer, C.G., and C.A. McGugan. 1988. Investigation of Enthalpy Residential Air-to-Air Heat Exchangers. Final Report for ASHRAE Research Project RP-544 (Report No.EEE/ESC-88-08).

Carll, C., A. TenWolde, and R. Munson. 2007. Moisture performance of a contemporary wood-frame house operated at design indoor humidity levels. *Proceedings of the Thermal Peformance of the Exterior Envelopes of Whole Buildings X Conference, Atlanta, USA.*

Christian, J.E. 2009. *Moisture Control in Buildings, 2nd Ed.* Chapter 7, "Moisture Sources." H.R. Trechsel and M.T. Bomberg, Eds. West Conshohocken, PA: ASTM International.

FTF. 1999. The Foundation Test Facility (FTF). http://www.buildingfoundation.umn.edu/ftf.htm#@FTF_1, accessed April 2010.

Glass, S.V., and A. TenWolde. 2009. Review of moisture balance models for residential indoor humidity. *Proceedings of the 12th Canadian Conference on Building Science and Technology,* 1:231-45.

Gueymard, C.A., and D. Thevenard 2009. Monthly average clear-sky broadband irradiance database for worldwide solar heat gain and building cooling load calculations. *Solar Energy* 83: 1998–2018.

Hollinger, S.E., and S.A. Isard. 1994. A soil moisture climatology of Illinois. *Journal of Climate* 7:822–33.

IBP. 2009. WUFI Pro 4.2. www.wufi.de/index_e.html. Holzkirchen, Germany: Fraunhofer Institute for Building Physics.

Kalamees, T., J. Vinha, and J. Kumitski. 2006. Indoor humidity loads and moisture production in lightweight timer-frame detached houses. *Journal of Building Physics* 29:219-46.

Kumaran, K., and C. Sanders. 2008. IEA Annex 41: Whole building heat, air, moisture response, Subtask 3: Boundary conditions and whole building HAM analysis. International Energy Agency, Executive committee on Energy Conservation in Buildings and Community Systems.

Kumitski, J., T. Kalamees, J. Palonen, L. Eskola, and O. Seppanen. 2007. Potential effects of permeable and hygroscopic lightweight structures on thermal comfort and perceived IAQ in a cold climate. *Indoor Air* 17:37-49.

Plathner, P., J. Littler, and A. Cripps. 1998. Modeling water vapor conditions in dwellings. *Third International Symposium on Humidity and Moisture, London, UK,* 2:64–72.

Quirouette, R.L. 1983. Moisture Sources in Houses. *Building Science Insight '83.* Division of Building Research, National Research Council of Canada.

Robock, A., K.Ya. Vinnikov, G. Srinivasan, J.K. Entin, S.E. Hollinger, N.A. Speranskaya, S. Liu, and A. Namkhai. 2000. The global soil moisture data bank. *Bull. Amer Meteor. Soc.* 81:1281–99.

TenWolde, A. 1994. Ventilation, humidity, and condensation in manufactured houses during winter. *ASHRAE Transactions* 100:103–15.

TenWolde, A., and I.S. Walker. 2001. Interior moisture design loads for residences. *Proceedings of Performance of the Exterior Envelopes of Whole Buildings VIII, Atlanta, USA.*

TenWolde, A., and C. Pilon. 2007. The effect of indoor humidity on water vapor release in homes. *Proceedings of Thermal Performance of the Exterior Envelopes of Whole Buildings X, Atlanta, USA.*

Walker, I.S., and D.J. Wilson. 1998. Field validation of algebraic equations for stack and wind driven air infiltration calculations. *HVAC&R Research* 4(2): 119–39.

Wang, W., I. Beausoleil-Morrison, and J. Reardon. 2009. Evaluation of the Alberta air infiltration model using measurements and inter-model comparisons. *Building and Environment* 44:309–18.

Boardman, C.R., Glass, S.V., Carll, C.G.: *Estimating Foundation Water Vapor Release Using a Simple Moisture Balance and AIM-2: Case Study of a Contemporary Wood-Frame House.*
Thermal Performance of the Exterior Envelopes of Whole Buildings XI International Conference, December 5-9, 2010, Clearwater Beach, Florida American Society of heating, Ventilating and Air-Conditionings Engineers, Inc. The ISBN 978-1-933742-89-2; 2010